Journal of Materials Chemistry C

Accepted Manuscript

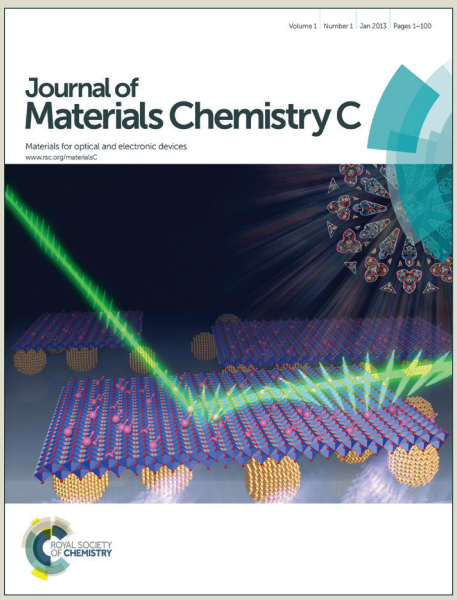

ROYAL SOCIETY OF CHEMISTRY

www.rsc.org/materialsC

Journal Name

RSC Publishing

ARTICLE

Optical Sensor Based on Hydrogel Films with 2D Colloidal Arrays Attached on Both Surfaces: Anti-curling Performance and Enhanced Optical Diffraction Intensity

Cite this: DOI: 10.1039/x0xx00000x

Received 00th January 2012,
Accepted 00th January 2012

DOI: 10.1039/x0xx00000x

www.rsc.org/

Dandan Men[a,b], Honghua Zhang[a,b], Lifeng Hang[a,b], Dilong Liu[a,b], Xinyang Li[a], Weiping Cai[a] Qihua Xiong[c] and Yue Li[a,b*]

An interesting strategy to create free standing hydrogel composite films with colloidal monolayers attached on both of their surfaces is developed, which could be acted as visualized sensors with high diffraction intensity. Thanks to the balanced stress on their both surfaces, the colloidal monolayer/hydrogel composite films overcome curling problem of traditional hydrogel films loaded with colloidal monolayer on one side. They also display enhanced diffraction intensity than those with the attachment of only a single 2D colloidal monolayer due to multi-diffraction effect. Such sensing hydrogel composite films with anti-curling performance and enhanced optical diffraction intensity are highly helpful to improve their practical applications in visual and quantitative detection. Additionally, this strategy is universal and could be suitable for fabricating various functional hydrogel films loaded with different nanosphere arrays for novel optical sensors.

Introduction

Generally, chemical and biological agents are detected by some complicated techniques before they achieve dangerous levels, such as Raman spectroscopy, high-performance liquid chromatography and gas chromatography. These techniques are costly and time-consuming, which limit their practical utilities[1,2]. Therefore, there is a strong demand to develop alternative methods to detect chemical and biological species with low cost and a simple operation. In particularly, visual detection is popular and attractive due to its display of existence of dangerous molecules in a short time, which can be directly observed by naked eyes. It is generally based on a rapid optical response for analytes[3-12]. Among the various kinds of visualized detecting technologies, some reports focused on using responsive photonic crystals (PCs) as chemical and biological sensors to detect target analytes by different visible colors due to changed optical diffraction for various periodicities of responsive PCs[3]. Specifically, hydrogel photonic crystals (HPCs) can be tailored to respond to various external stimuli, such as humidity[4], temperature[5], organic solvents[6], pH values[7,8], 3-Pyridinecarboxamide[13], pressure[10], glucose[14-20], ionic strength[9] and metal ions[1,21], but without structural destruction. Therefore, HPCs are good candidates to be developed optical sensors for various external stimuli. The visual optical diffraction can be discovered once an external stimulus is applied[22].

In past years, HPCs have been developed by embedding three dimensional (3D) colloidal crystals into the functional hydrogel films[23,24]. The volume change of the hydrogel in response to stimuli would be converted into the diffracted wavelength-shift. However, the self-assembly of 3D colloidal crystals is time-consuming because it usually takes several weeks to obtain a good ordered structure. Another disadvantage is that the functionalization of hydrogel precursors must be homogeneous in order to avoid destroying the 3D arrays, limiting their further applications. Recently, there has been growing interest in the fabrication of responsive PCs by using two dimensional (2D) colloidal arrays to prepare visualized sensors due to the facile manipulation and their rapid response to external stimuli[1,2,25-27]. Asher et al. investigated functional hydrogel films with 2D colloidal crystals attached onto one surface to allow the visualized detection to the chemical species including pH[1,25], amphiphilic molecules[2], avidin[26] and Pb^{2+}[27]. Such 2D colloidal crystal/functional hydrogel composite films are intrinsically more sensitive than those only relied on refractive index changes. Because a change of the hydrogel volume can give rise to very large alteration of microsphere interspacing in the 2D arrays, but the refractive index induced by external stimuli can be only changed in a very small range, leading to the limited change in optical diffraction[22]. However, it still keeps a challenge to achieve the 2D

array/hydrogel films with high diffraction intensity without curling to be used as effective visualized sensors.

Compared with traditional 3D colloidal crystal/hydrogel composites, 2D colloidal crystal/hydrogel films have more advantages. Firstly, the self-assembly of 2D colloidal array at air-water interface is much simpler and faster than that of 3D one[28-33]. Secondly, such thin hydrogel composite film with micrometer-thickness allows rapid detection because of rapid diffusion of target agents, resulting in high sensitivity[1]. Thirdly, the preparation of 3D colloidal array/hydrogel composite strictly requires use of non-ionic hydrogel precursors in order to get a good periodicity[26], but there is no such requirement to synthesize 2D colloidal array/hydrogel film, but making 2D arrays keep well ordering. However, for 2D array/hydrogel composite films with 2D colloidal crystals attached only on one surface, the unbalanced stress existed on both surfaces (top and bottom surfaces) makes the composite films to be easily curly. Additionally, such 2D array/hydrogel composites demonstrate relatively low diffraction intensity. These facts seriously obstruct their practical applications as effective sensors.

Herein, we develop an interesting strategy to prepare free standing colloidal crystal/hydrogel film with 2D colloidal crystals attached on both surfaces (top and bottom surface). Such hydrogel composite films can overcome curling problem of traditional hydrogel films loaded with colloidal monolayer on one side, when it suffered from various external stimuli of target agents due to uniform stress on top and bottom surfaces of hydrogel film, producing the flat samples without curling, which is useful to visual observation by naked eyes and further optical characterization. More importantly, the hydrogel films with 2D monolayer arrays attached on both surfaces demonstrate much stronger diffraction intensity than those with the attachment of only a single 2D colloidal monolayer to external stimuli, which is highly helpful to improve their practical applications in visual and quantitative detection by monitoring the diffraction peak position and intensity. This synthesizing route is universal and could be used to various functional hydrogel films and different nanosphere arrays for novel optical sensors. Here, taking chitosan hydrogel films with PS colloidal monolayers loaded on their both surfaces to response to pH as an example, we show that free standing colloidal crystal/hydrogel composite sensing films can be formed by the strategy presented in this paper.

Experimental

Materials

Polystyrene (PS) microspheres with diameter of 500 nm were purchased from Alfa Aesar Corporation. Chitosan (CS) (deacetylation degree %: 80-95%), glutaraldehyde, methylenedichloride, sodium hydroxide, boric acid, phosphoric acid and acetic acid were obtained from Sinopharm Chemical Reagent Corporation Ltd. They were directly used without further purification. Water (18.2 MΩ.cm) was obtained from an ultrafiter system (Milli-Q, Millipore, Marlborough, MA).

Preparation of CS solution. CS with a certain mass was dissolved in 1 wt% acetic acid aqueous solution to make a 2 wt% CS solution. After complete dissolution of CS, 20 μL glutaraldehyde was added into the 20 mL 2 wt% CS solution in order to cross-link the CS.

Preparation of 2D PS colloidal monolayer. The 2D PS colloidal monolayer was prepared on a cleaned glass slide by an air-water interfacial self-assembly method, as reported previously[34-37]. Briefly, the PS aqueous suspension and alcohol were mixed at a ratio of 1:1 and this mixture was vortexed for 10 min. An appropriate amount of deionized water was dropped and covered on a cleaned glass slide surface. Then a droplet of PS suspension was dropped onto the water surface, 2D PS colloidal monolayer was fabricated by self-assembly at air-water interface, finally, it would stay on glass substrates after complete evaporation of water film at room temperature.

Preparation of CS hydrogel films with 2D PS colloidal crystals embedded into both surfaces. CS hydrogel film with 2D PS colloidal crystals attached on both surfaces was prepared by attaching 2D PS colloidal arrays onto both surfaces of CS hydrogel film (Fig. 1). Firstly, 100 μL of 2 wt% polyvinyl alcohol (PVA) was firstly spin-coated on a cleaned glass slide at spin speed of 1800 rpm (Fig. 1a). Subsequently, a 2D colloidal monolayer was transferred onto PVA/glass substrate using water surface as a media[38,39] (Fig. 1b). Another colloidal monolayer was then transferred on such colloidal crystal/PVA/glass substrate using the same route (Fig. 1c). Then a certain amount of 2 wt% CS solution was cast into double layered colloidal crystals on the PVA/glass slide, the top colloidal monolayer was lifted and floated on CS solution film, but 2D colloidal crystal on the bottom still attached the PVA/substrate because of the high adhesion of PVA (Fig. 1d). As a result, the CS hydrogel film with 2D PS colloidal crystals attached on both surfaces was fabricated after the 2D colloidal crystal/ hydrogel composite film dried at room temperature and was peeled off the glass substrate (Fig. 1e). Finally, the dried CS film coated with colloidal monolayer on the top and bottom surfaces was treated with a 0.2 M NaOH aqueous solution to neutralize the remaining acetic acid and then washed repeatedly with deionized water. As a comparison, the CS hydrogel film with 2D PS colloidal crystal attached only on one surface was also fabricated.

Characterization

The morphology of the as prepared samples were characterized by a field-emission scanning electron microscope (FESEM, Sirion200) after coated an Au thin layer for good conduction. The measurements of diffraction spectra were conducted at a fixed angle utilizing an Idea Optics PG2000-Pro-EX Spectrometer, R1-A-UV Support and Halogen & Deuterium Light Source. Diffraction measurements were performed in the Littrow configuration by using two arms at the same direction. One arm excites white light and another arm collects the diffracted light with a semi-transparent mirror. The measurement angle between the probe and the normal direction to the samples is 36°. In the process of diffraction measurements, all 2D colloidal array/hydrogel composite films were placed on aluminum mirrors in order to increase diffraction intensity. To characterize the response of the 2D colloidal array/hydrogel composite films to pH, the as prepared samples were immersed in Britton-Robinson (B-R) buffer solution with different pH values (from 2.07 to 6.88). The 2D array/hydrogel composite films were equilibrated overnight before diffraction measurements.

Results and discussion

2D colloidal crystals/hydrogel composite films

Generally, a rapid response to the external environment of sensing materials and their good mechanical stability are key factors in their practical applications[6]. In this work, we chose CS hydrogel film due to its diffusion property and its robust structure[40]. Additionally, the use of glutaraldehyde as a cross-linking agent to make CS into a chemical cross-linked 3D hydrogel network can well improve mechanical stability[41,42]. Hydrogel film with 2D PS arrays attached on both surfaces was fabricated by attaching 2D PS arrays with a diameter of 500 nm to both surfaces of CS hydrogel film, as shown in Fig. 1 (detailed information can be found in Experimental Section).

Fig. 2 illustrates FESEM images of hydrogel film with 2D PS

colloidal arrays attached on both surfaces. Fig. 2a shows a cross-sectional image of the as prepared colloida monolayer/hydrogel composite film, indicating the 2D PS monolayer arrays mounted on its both surfaces. The corresponding SEM images of 2D colloidal arrays on the top and bottom surface of hydrogel film were displayed in Fig. S1a and Fig. S1b (Supporting Information), respectively. It showed that the monolayer colloidal crystal demonstrated a hexagonal-close-packed arrangement and the spaces between neighboring colloidal spheres were filled with hydrogel polymer. The 2D hole arrays could be found after dissolving PS colloidal spheres attached on surfaces of the CS hydrogel film by methylenedichloride, as shown in Fig. S1c, further proving that the CS solution infiltrated the interstices among colloidal spheres in an array and colloidal spheres were really embedded in the hydrogel film. Additionally, as a comparison, a CS hydrogel film loaded with a 2D PS colloidal array only on top surface was also prepared (Fig. S2). Both 2D colloidal crystals/hydrogel composite films with colloidal monolayers on both surfaces and only on top surface displayed iridescent colors, indicating the formation of periodic colloidal arrays on their surfaces. The thickness of the CS hydrogel film loaded with the colloidal crystals on both surfaces was ca. 8 μm. Fig. 2b shows a photograph of CS hydrogel with 2D arrays attached on both surfaces and only on one surface in water at the same time, respectively. It clearly shows the CS hydrogel loaded with 2D array on one surface is curly, but the film with 2D colloidal arrays attached on both surfaces is much flatter. So, the attachment of 2D arrays on both surfaces of hydrogel films could improve their anti-curly degree duo to the balance stress on both surfaces of hydrogel film. Such flat 2D array/hydrogel composite films are highly helpful for their further applications as sensors.

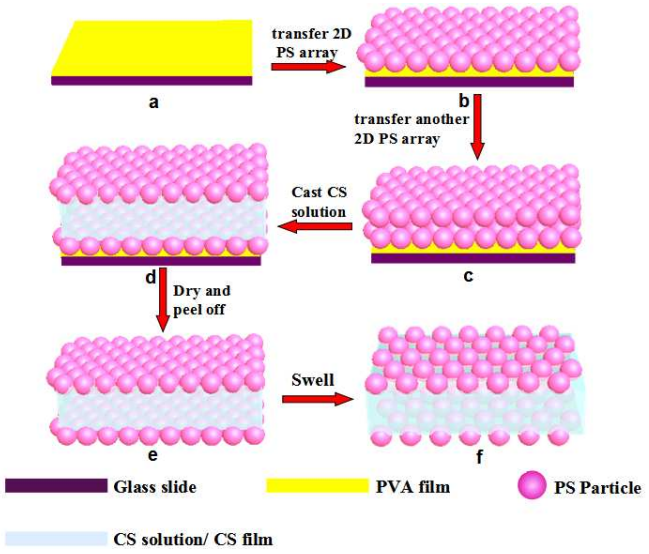

Fig. 1. Preparation of CS hydrogel film with 2D colloidal arrays attached on both surfaces: a. A PVA thin film was prepared on a cleaned glass slide surface by spin coating; b. A 2D PS colloidal array was transferred on PVA/glass slide; c. Another 2D colloidal crystal array was transferred on colloidal crystal array/PVA/glass slide; d. CS solution was cast on colloidal arrays; e. A free standing 2D array/CS hydrogel composite film was obtained by peeling it off glass slide; f. The 2D array/CS hydrogel composite film was swelled responding to external stimuli of pH.

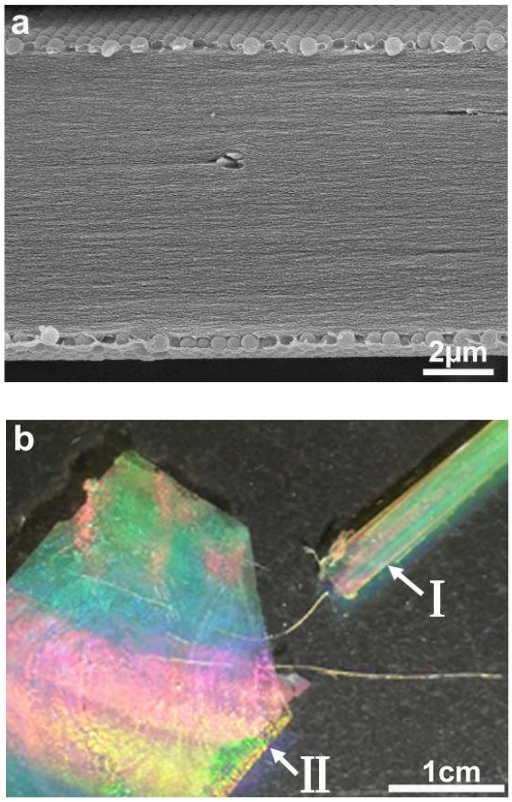

Fig. 2. SEM images of (a) Cross-section of 2D colloidal arrays/hydrogel composite film with 2D PS arrays attached on the both surfaces; (b) Photograph of CS hydrogel films loaded with 2D array in both surfaces (II) and one surface (I) in water.

Enhanced optical diffraction intensity

Bragg diffraction generally occurs when light with certain wavelength illuminate the corresponding matched periodic structures. The diffraction of the 2D periodic array can be calculated by the following formula, $m\lambda = \sqrt{3}d\sin\theta$, where m is the diffraction order, λ is the diffraction wavelength, d is the nearest spacing of neighboring colloidal spheres in an array, and θ is the angle between the incident light and the normal direction of the periodic array[2,43]. Hence, the peak position of diffracted wavelength could be largely changed due to changes of the nearest spacing of neighboring spheres caused by volume swelling or shrinking of the functional hydrogel carrier.

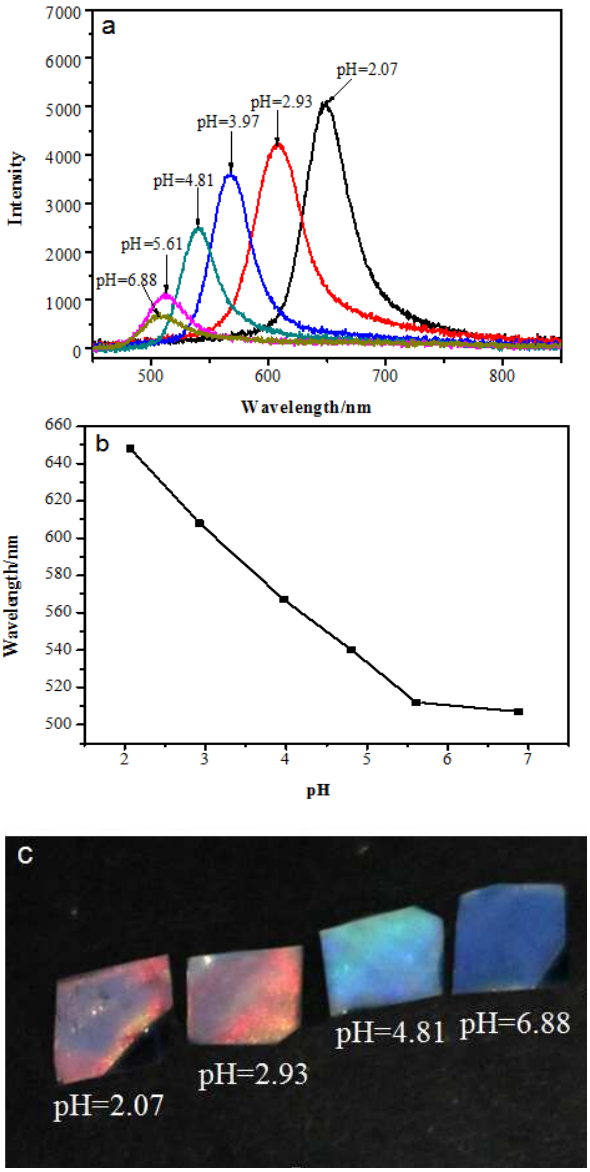

Fig. 3. (a) Diffraction spectra of CS hydrogel film with 2D arrays on both surfaces at pH: 2.07, 2.93, 3.97, 4.81, 5.61 and 6.88; (b) pH dependence of the diffraction wavelength of as-prepared colloidal monolayer/hydrogel films after equilibration in different pH buffer solutions; (c) corresponding photographs of 2D array hydrogel films loaded with 2D array on both surfaces at pH: 2.07, 2.93, 4.81 and 6.88.

Fig. 3 shows the diffraction spectra with single peaks of the hydrogel sensor wtih 2D PS arrays on both surfaces at B-R buffer solution with different pH values. At pH 6.88, a diffraction peak centered at 508 nm is observed, which is in good agreement with the data (509 nm) of unswelled hydrogel film loaded with colloidal crystals, calculated by the Bragg diffraction formula. It indicates the colloidal crystal array/hydrogel composite film is not swelled at pH 6.88 due to neutralization of the NH_2 groups. However, with decrease of pH value, the diffraction peak is red-shifted gradually. It shifted to 648 nm when pH value decreased to 2.07. The red shift is caused by the increased PS sphere interspacing due to ionization of NH_2 groups. Ionization of NH_2 groups immobilizes counterions inside the hydrogel results in an osmotic pressure of the polymeric network inside and outside[9] and it also leads to producing electrostatic repulsive force among protonated amino groups in CS[44]. Additionally, the association of hydrogen bond between NH_2 groups were weakened with the ionization of NH_2 groups, making chain segment motions of the polymer become much easier[45]. Hydrogel films were swelled by all above factors and the swelling of hydrogel made interspacing between PS spheres increase in colloidal monolayer arrays embedded in its surfaces. The increased interspacing would cause the red-shift of diffracted wavelength and the color change, according Bragg diffraction formula. A decreased pH value increases the number of protonated NH_2 groups in the hydrogel, leading to a higher swelling degree, further resulting in a larger interspacing of colloidal spheres that loaded on hydrogel film and a larger diffraction red-shift in optical response. The pH dependence of the diffraction peak position of colloidal monolayer array/hydrogel composite films loaded with 2D PS arrays on both surfaces at B-R buffer solution with different pH values was showed in Fig. 3b. It indicates that the intensity of diffraction peak decreased significantly with increase of pH value. Furthermore, an obvious color change of 2D PS arrays loaded on hydrogel films can be clearly observed by naked eyes under different pH values, as demonstrated in Fig. 3c. One can find it changed from rouge noir to red, then to cyan, and finally to blue with increase of pH value. Therefore, the as-prepared colloidal arrays/hydrogel composite film could be used as a sensor for fast and visual detection of pH value via color changes. As a comparison, the 2D PS array/CS hydrogel film with colloidal array attached only on top surface was also prepared. Fig. S3 displays its diffraction spectra at B-R buffer solution with different pH values. It shows a similar optical behavior with colloidal monolayer array/CS hydrogel composite film with 2D array on both surfaces. With decrease of pH value from 6.88 to 2.07, the diffraction peak of CS hydrogel film with colloidal monolayer array on one surface was red-shifted from 509 to 692 nm. The larger shift of the diffraction (509 to 691 nm) of hydrogel film with 2D array on one surface compared to that with 2D arrays on both surfaces (508 to 648 nm) indicates the 2D arrays embedded in both surfaces of hydrogel film might restrain the swelling degree. Compared to the hydrogel film with 2D colloidal monolayer on one surface, 2D arrays loaded on both surfaces of hydrogel film would decrease diffusion of hydrogen ions in hydrogel matrix to some extent, further leading the lower ionization of NH_2 groups and welling degree of the hydrogel films.

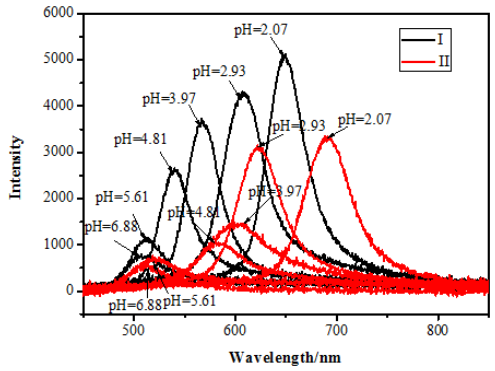

Fig. 4. Comparison of diffraction spectra of 2D arrays/CS hydrogel films with colloidal array on both surfaces (curve I) and one surface (curve II) at pH value: 2.07, 2.93, 3.97, 4.81, 5.61 and 6.88.

However, one can clearly find that the intensity of the diffraction peaks of hydrogel composite film with 2D colloidal arrays attached on both surfaces was much stronger than that of hydrogel composite film with monolayer colloidal array on one surface, as shown in Fig. 4. For example, the intensity of diffraction peak from the hydrogel composite film with 2D arrays on both surfaces was ca. 2.5 fold of that of hydrogel composite film with 2D array on one surface at pH 3.97. At higher pH value, hydrogel composite film with 2D array on both surfaces also increased the diffracted intensity, but not so much. Therefore, comparison of diffraction spectra of them at different values indicates that 2D arrays loaded on both hydrogel film surfaces can largely enhance diffraction intensity, which is highly helpful to develop a sensor for visual detection. Additionally, in order to reveal the thickness influence to diffraction intensity, we tried to prepare the CS hydrogel film with the colloidal crystals on both surfaces with different thickness of ca. 12, 8, 5 μm, respectively. Their diffraction spectra were measured at pH 2.07 (Fig. S4) and the diffraction intensity slightly decreased with increase of thickness of CS film, but the change of intensity is not very obvious with change of thickness of CS film.

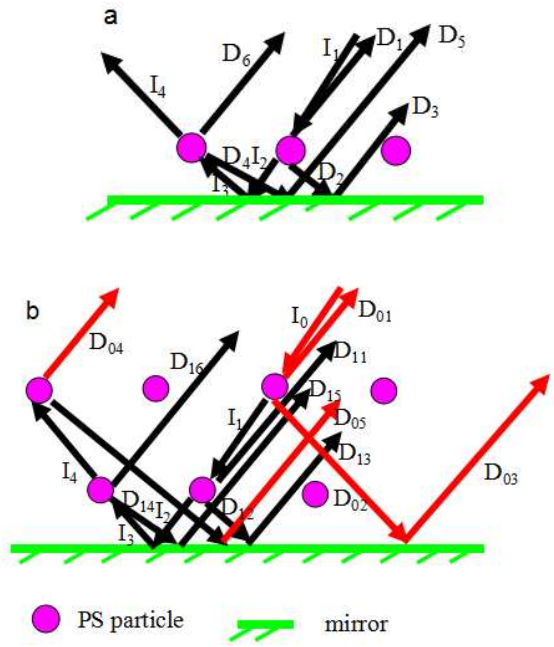

Fig. 5. Diffraction illustration of 2D colloidal monolayer arrays/hydrogel composite films. (a) Diffraction of 2D array/CS hydrogel film with 2D array only on one surface from a mirror; (b) Diffraction of 2D array/CS hydrogel film with 2D arrays on both surfaces from a mirror.

We present a mechanism to explain the enhanced intensity of diffraction peaks of CS hydrogel film with 2D array on both surfaces. For the case of the 2D colloidal crystal/hydrogel composite film with monolayer colloidal array on one surface, the incident light (I_1) on the 2D colloidal array firstly diffracts into back-diffracted beam D_1 and forward-diffracted beam D_2. D_2 is reflected by mirror to form beam D_3. The transmitted light (I_2) of incident light is reflected by mirror to form I_3. This light gives rise to beam D_4 and beam D_6 due to the diffraction of 2D array. Beam D_4 is reflected to form beam D_5. D_1, D_3, D_5 and D_6 are parallel to each other and they can be detected or observed from the incident direction[1,46]. Therefore, the total intensity of diffracted light to detector from the incident direction is a sum of D_1, D_3, D_5 and D_6, as demonstrated in Fig. 5a. Additionally, the transmitted light I_4 of I_3 will not be collected on the incident side due to the different direction. However, for the case of the 2D array/hydrogel composite film with 2D monolayer colloidal arrays on both surfaces, the diffraction is a little different from that of hydrogel composite film with monolayer colloidal array on one surface, as displayed in Fig. 5b. In this case, the incident light (I_1) on 2D colloidal array embedded in the top surface of hydrogel will produce diffraction on the incident direction to form beam D_{01} and D_{03}. When the transmitted light I_2 of incident light illuminates the bottom 2D PS array under hydrogel film will give rise to diffraction again on the incident direction to form beam D_{11}, D_{15}, D_{13} and D_{16}. In contrast with the diffraction of hydrogel film with monolayer colloidal array only on top surface, the transmitted light I_4 from I_3 will be diffracted by the top layered 2D PS array to from beam D_{04} and D_{05} on the incident side. D_{01}, D_{03}, D_{11}, D_{15}, D_{13}, D_{16}, D_{05} and D_{04} are parallel to each other and they could be detected or observed from the incident direction. Therefore, the total intensity of diffracted light to detector from the incident direction is a sum of D_{01}, D_{03}, D_{11}, D_{15}, D_{13}, D_{16}, D_{05} and D_{04} for hydrogel composite films with colloidal arrays on their both surfaces, as shown in Fig. 5b. In

later case, more diffracted beams could be collected, resulting in the much stronger diffraction intensity. Thus, both integration of CS hydrogel films with 2D arrays on both surfaces with improving curly degree and enhancing diffraction intensity are helpful to visual observation by naked eyes and further optical characterization in their practical applications.

Conclusion

In summary, an interesting route to prepare free standing hydrogel composite films with colloidal monolayers on both surfaces is developed. They could be used as visualized sensors with high diffraction intensity. The as-prepared hydrogel composite films overcome curling problem of traditional hydrogel films loaded with colloidal monolayer on one side, when they suffered from various external stimuli of target agents owing to uniform stress on the top and bottom surfaces, leading to the flat samples without curling. More importantly, they display much stronger diffraction intensity than those with colloidal monolayer on one surface to external stimuli due to multi-diffraction effect. The anti-curling performance and enhanced optical diffraction intensity of sensing hydrogel films with 2D colloidal arrays on both surfaces are highly helpful to improve their practical applications in visual and quantitative detection by monitoring the diffraction peak position and intensity. Additionally, this presented strategy is universal and could be suitable for various functional hydrogel and different nanosphere arrays for new optical sensors.

Acknowledgements

The authors acknowledge the financial support from the National Basic Research Program of China (Grant No. 2012CB932303), Recruitment Program of Global Experts (C), Natural Science Foundation of China(Grant Nos. 51371165), Cross-disciplinary Collaborative Teams Program in CAS, the CAS/SAFEA International Partnership Program for Creative Research Teams.

Notes and references

[a] Institute of Solid State Physics, Chinese Academy of Sciences, Hefei, 230031, P. R. China
[b] Department of Materials Science and Engineering, University of Science and Technology of China, Hefei, 230026, P. R. China
E-mail: yueli@issp.ac.cn
[c] School of Physical and Mathematical Sciences, Nanyang Technological University, Singapore

Electronic Supplementary Information (ESI) available: [details of any supplementary information available should be included here]. See DOI: 10.1039/b000000x/

1 J. T. Zhang, L. L. Wang, J. Luo, A. Tikhonov, N. Kornienko and S. A. Asher, *J. Am. Chem. Soc.,* 2011, **133**, 9152-9155.
2 J. T. Zhang, N. Smith and S. A. Asher, *Anal. Chem.,* 2012, **84**, 6416-6420.
3 C. Fenzl, T. Hirsch and O. S. Wolfbeis, *Angew. Chem. Int. Ed.,* 2014, **53**, 3318-3335.
4 E. T. Tian, J. X. Wang, Y. M. Zheng, Y. l. Song, L. Jiang and D. B. Zhu, *J. Mater. Chem.,* 2008, **18**, 1116-1122.
5 J. H. Kang, J. H. Moon, S. K. Lee, S. G. Park, S. G. Jang, S. Yang and S. M. Yang, *Adv. Mater*., 2008, **20**, 3061-3065.
6 J. Y. Wang, Y. Cao, Y. Feng, F. Yin and J. P. Gao, *Adv. Mater.* 2007, **19**, 3865-3871.
7 E. T. Tian, Y. Ma, J. X. Wang, Y. L. Song and L. Jiang, *Macromol. Rapid Commun.,* 2009, **30**, 1719-1724.
8 Y. J. Lee, P. V. Braun, *Adv. Mater*., 2003, **15**, 563-566.
9 K. Lee, S. A. Asher. *J. Am. Chem. Soc*., 2000, **122**, 9534-9537.
10 S. H. Foulger, P. Jiang, A. C. Lattam, D. W. Smith and J. Ballato, *Langmuir*, 2001, **17**, 6023-6026.
11 H. H. Cheng, J. Liu, Y. Zhao, C. G. Hu, Z. P. Zhang, N. Chen, L. Jiang and L. T. Qu, *Angew. Chem. Int. Ed*., 2013, **52**, 10482-10486.
12 H. Bai, C. Du, A. J. Zhang, and L. Li, *Angew. Chem. Int. Ed*., 2013, **52**, 12240-12255.
13 Y. X. Yuan, Z. L. Li, Y. Liu, J. P. Gao, Z. Pan and Y. Liu, *Chem. Eur. J.,* 2012, **18**, 303-309.
14 C. J. Zhang, M. D. Losego, and P. V. Braun, *Chem. Mater.,* 2013, **25**, 3239-3250.
15 D. Nakayama, Y. Takeoka, M. Watanabe and K. Kataoka, *Angew. Chem. Int. Ed.,* 2003, **42**, 419-4200.
16 V. L. Alexeev, A. C. Sharma, A. V. Goponenko, S. Das, I. K. Lednev, C. S. Wilcox, D. N. Finegold and S. A. Asher, *Anal. Chem.,* 2003, **75**, 2316-2323.
17 C. J. Zhang, G. G. Cano and P. V. Braun, *Adv. Mater.,* 2014, **26**, 5678-5683.
18 S. A. Asher, V. L. Alexeev, A. V. Goponenko, A. C. Sharma, I. K. Lednev, C. S. Wilcox and D. N. Finegold, *J. Am. Chem. Soc.,* 2003, **125**, 3322-3329.
19 Y. J. Lee, S. A. Pruzinsky and P. V. Braun, *Langmuir,* 2004, **20**, 3096-3106.
20 V. L. Alexeev, S. Das, D. N. Finegold and S. A. Asher, *Clin. Chem.,* 2004, **50**, 2353-2360.
21 A. V. Goponenko, S. A. Asher, *J. Am. Chem. Soc.,* 2005, **127**, 10753-10759.
22 J. P. Ge, Y. D. Yin, *Angew. Chem. Int. Ed.,* 2011, **50**, 1492-1522.
23 A. C. Sharma, T. Jana, R. Kesavamoorthy, L. Shi, M. A. Virji, D. N. Finegold and S. A. Asher, *J. Am. Chem. Soc.,* 2004, **126**, 2971-2977.
24 M. B. Moshe, V. L. Alexeev and S. A. Asher, *Anal. Chem.,* 2006, **78**, 5149-5157.
25 J. T. Zhang, L. L. Wang, D. N. Lamont, S. S. Velankar and S. A. Asher, *Angew. Chem. Int. Ed.,* 2012, **51**, 6117-6120.
26 J. T. Zhang, X. Chao, X. Y. Liu and S. A. Asher, *Chem. Commun.,* 2013, **49**, 6337-6339.
27 J. T. Zhang, L. L. Wang, X. Chao and S. A. Asher, *Langmuir,* 2011, **27**, 15230-15235.
28 F. Xue, Z.H. Meng, F. Y. Wang, Q. H. Wang, M. Xue and Z. B. Xu, *J. Mater. Chem. A.,* 2014, **2**, 9559-9565.
29 L. Li, T. Y. Zhai, H. B. Zeng, X. S. Fang, Y. Bando and D. Golberg. *J. Mater. Chem.,* 2011, **21**, 40-46.
30 S. Y. Lee, S. H. Kim, M. P. Kim, H. C. Jeon, H. Kang, H. J. Kim, B. J. Kim and S. M. Yang, *Chem. Mater.,* 2013, **25**, 2421-2426.
31 J. G. Cai, J. F. Ye, S. Chen, X. W. Zhao, D. Y. Zhang, S. Chen, Y. R. Ma, S. Jin and L. M. Qi, *Energy Environ. Sci.,* 2012, **5**, 7575-7581.
32 H. T. Yang, P. Jiang, *Langmuir,* 2010, **26**, 12598-12604.
33 Y. F. Li, J. H. Zhang and B. Yang, *Nano Today,* 2010, **5**, 117-127.
34 J. J. Wang, G. T. Duan, G. Q. Liu, Y. Li, Z. F. Dai, H. W. Zhang and W. P. Cai, *J. Mater. Chem.,* 2011, **21**, 8816-8821.

35 Y. Li, N. Koshizaki and W. P. Cai, *Coord. Chem. Rev.,* 2011, **255**, 357-373.
36 Y. Li, G. T. Duan, G. Q. Liu and W. P. Cai, *Chem. Soc. Rev.,* 2013, **42**, 3614-3627;
37 H. B. Zeng, X. J. Xu, Y. Bando, U. K. Gautam, T. Y. Zhai, X. S. Fang, B. D. Liu and D. Golberg, *Adv. Funct. Mater.,* 2009, **19**, 3165-3172.
38 Z. F. Dai, L. Xu, G. T. Duan, T. Li,H. W. Zhang, Y. Li, Y. Wang, Y. L. Wang, and W. P. Cai, *Sci. Rep.,* 2013, **3**, 1669.
39 Y Li, E. J. Lee and S. O. Cho, *J. Phys. Chem. C.,* 2007, **111**, 14813-14817.
40 J. Wu, M. J. Sailor, *Adv. Funct. Mater.,* 2009, **19**, 733-741.
41 M. M. W. Muscatello, S. A. Asher, *Adv. Funct. Mater.,* 2008, **18**, 1186-1193;
42 M. C. Du, Y. M. Zhu, L. H. Yuan, H. Liang, C. C. Mou, X. R. Li, J. Sun, Y. Zhuang, W. Zhang, Q. Shi, B. Chen and J. W. Dai, *Colloids and Surfaces A: Physicochem. Eng. Aspects.,* 2013, **434**, 78-87.
43 T. Kanai, T. Sawada and K. Kitamura. *Langmuir,* 2003, **19**, 1984-1986.
44 J. H. Kim, T. R. Lee, *Chem. Mater.,* 2004, **16**, 3647-3651.
45 Y. H. Shen, X. Y. Zhang, J. J. Lu, A. Q. Zhang, K. Chen and X. Q. Li, *Colloids and Surfaces A: Physicochem. Eng. Aspects.,* 2009, **350**, 87-90.
46 A. Tikhonov, N. Kornienko, J. T. Zhang, L. L. Wang and S. A. Asher, *J. Nanophotonics.,* 2012, **6**, 063509.

TOC figure